

Supplementary Information

Human-induced changes in the global meridional overturning circulation are emerging from the Southern Ocean

Sang-Ki Lee^{1*}, Rick Lumpkin¹, Fabian Gomez^{2,1}, Stephen Yeager³, Hosmay Lopez¹, Filippos Takglis^{4,1}, Shenfu Dong¹, Wilton Aguiar^{4,1}, Dongmin Kim^{4,1}, and Molly Baringer¹

¹NOAA Atlantic Oceanographic and Meteorological Laboratory, Miami, FL, USA

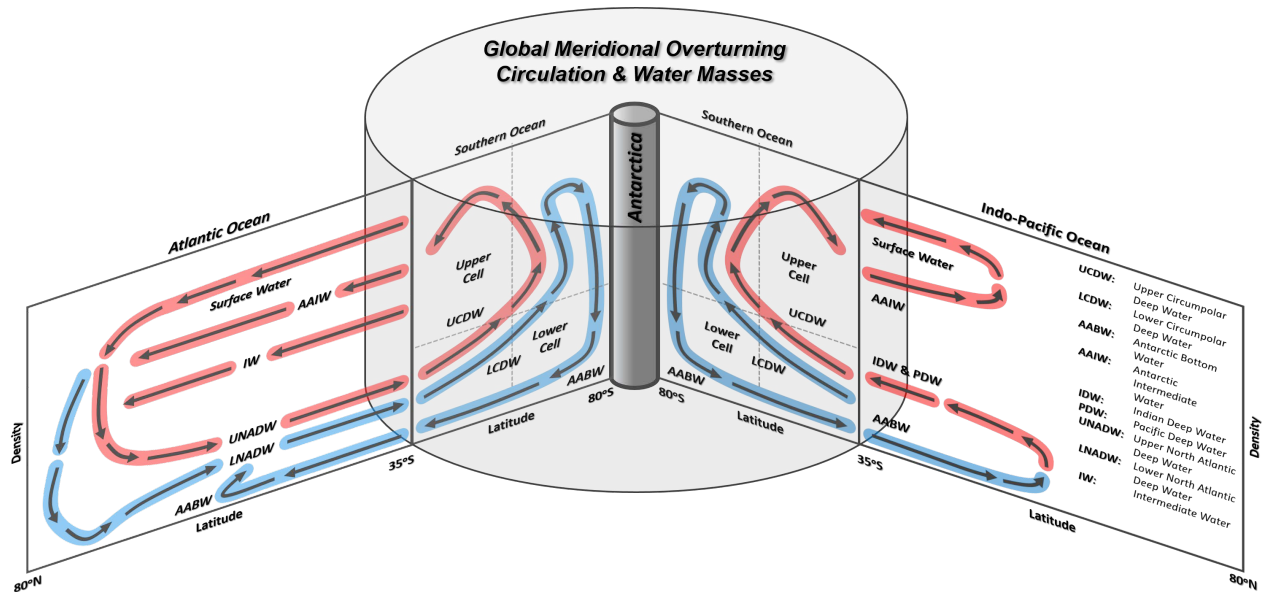
²Northern Gulf Institute, Mississippi State University, Mississippi State, MS, USA

³National Center for Atmospheric Research, Boulder, CO, USA

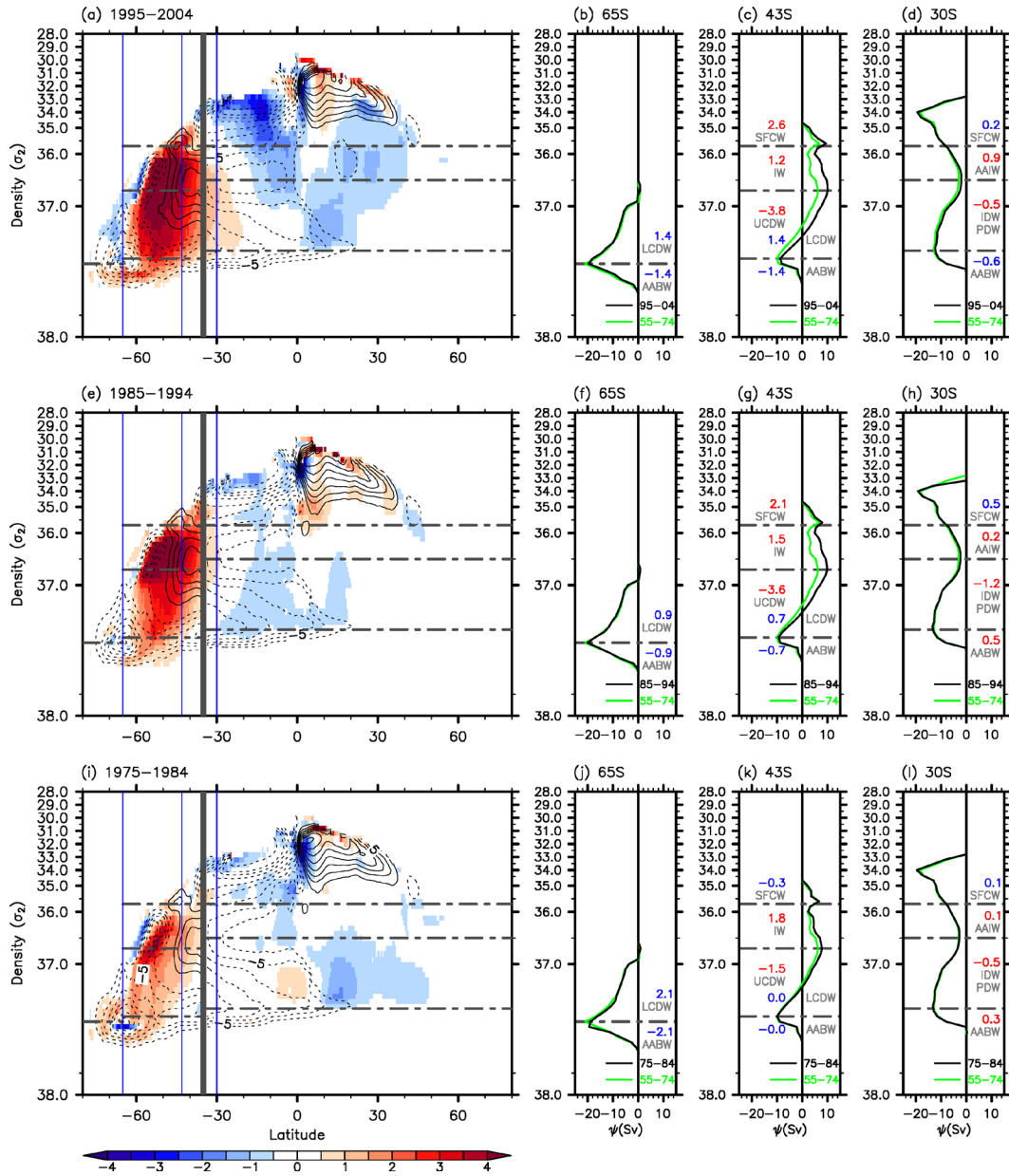
⁴Cooperative Institute for Marine and Atmospheric Studies, University of Miami, Miami, FL, USA

*Corresponding author: sang-ki.lee@noaa.gov

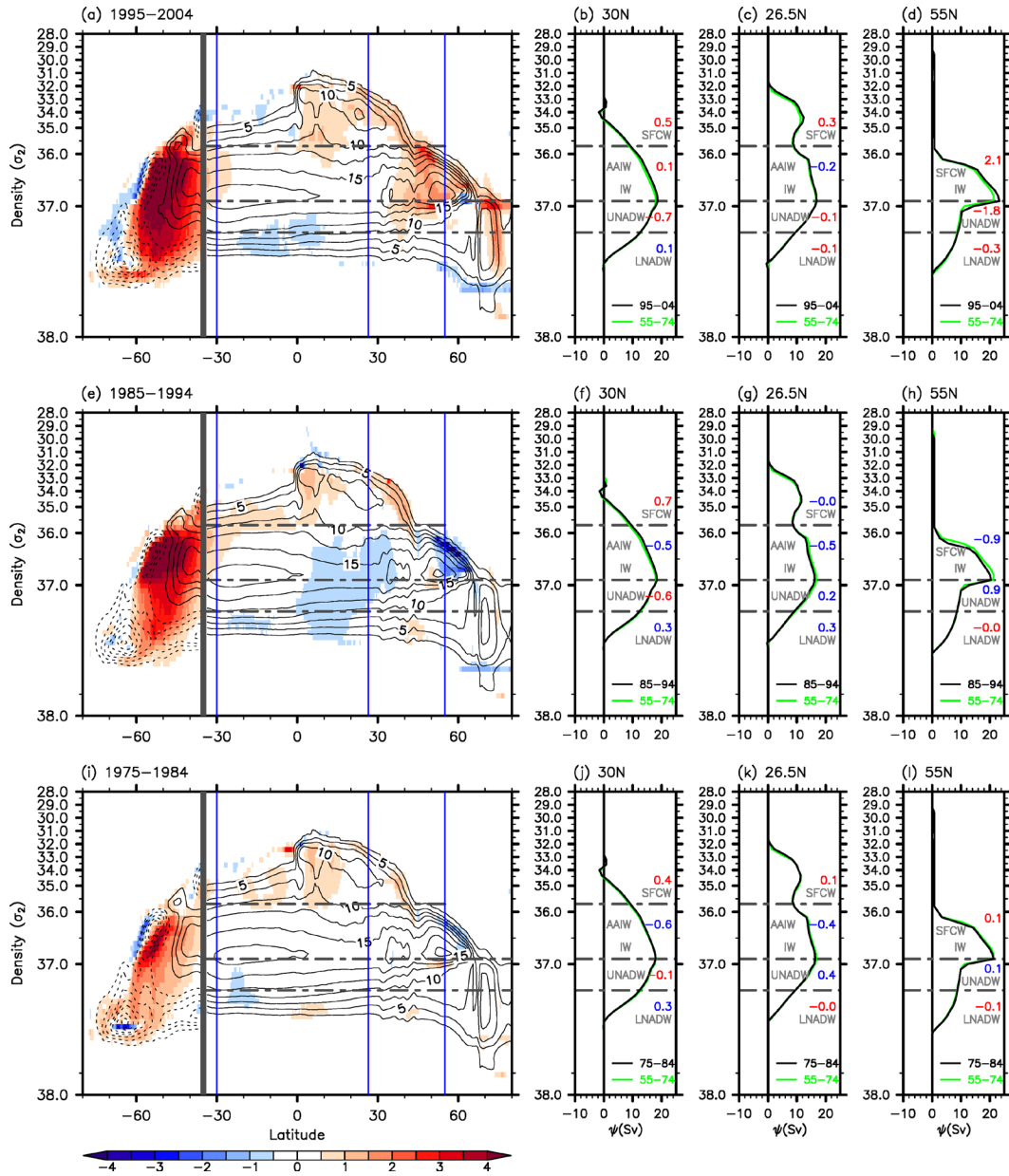
Communications Earth & Environment



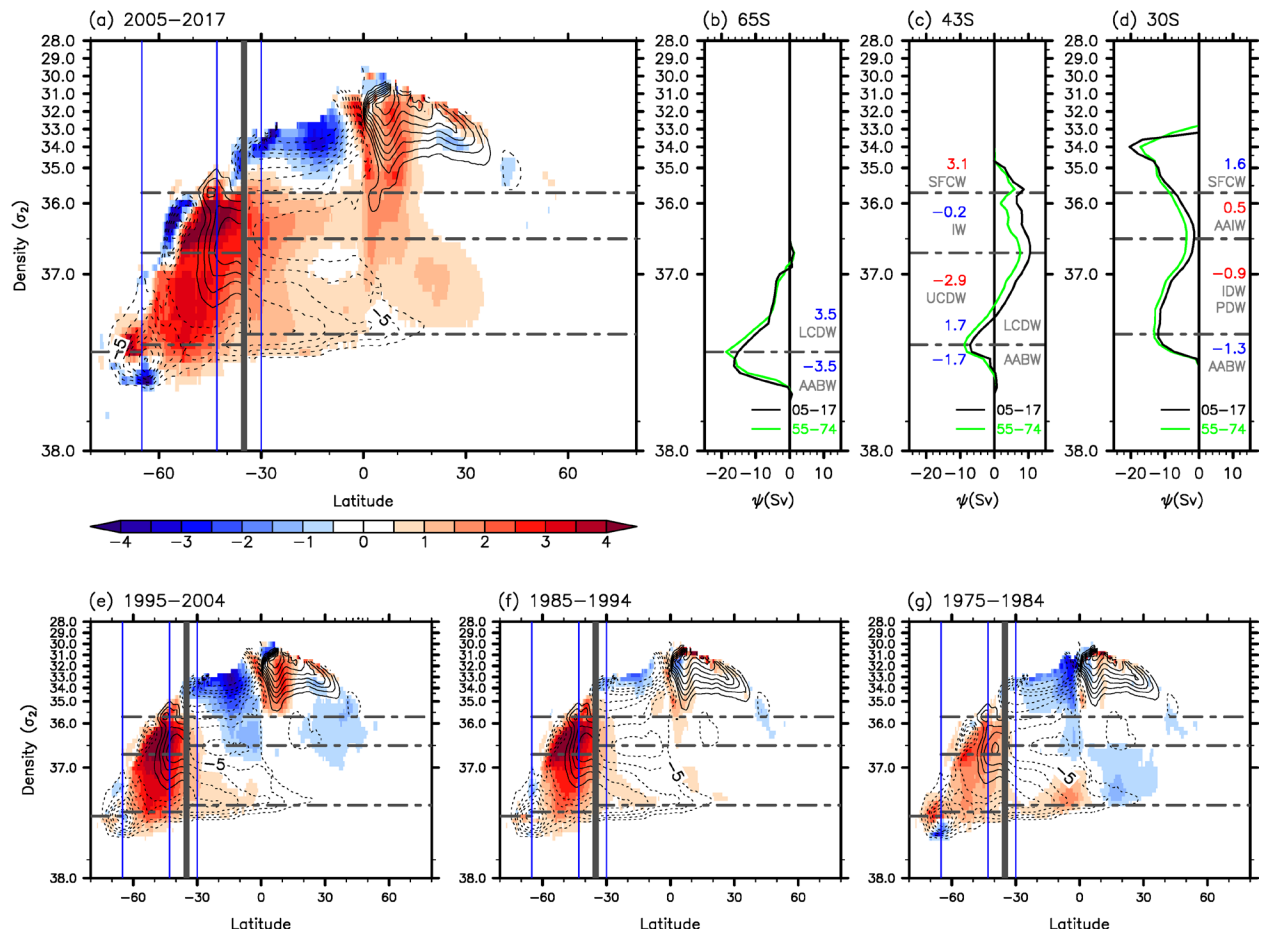
Supplementary Figure 1. The GIOC and water masses. A schematic of the GIOC in the Southern Ocean (south of 35°S), the Indo-Pacific Ocean and the Atlantic Ocean (north of 35°S) and the water masses referenced in this study^{44,47,48}. Note that AAIW refers to both Antarctic Intermediate Water and Sub-Antarctic Mode Water. Arrows with red shade indicate the transports contributing to the upper overturning cell, while those with blue shade indicate the transports contributing to the lower overturning cell. The vertical axis is density. This schematic illustrates the zonally integrated GIOC, and thus does not show the connections among different components of the GIOC within the Southern Ocean.



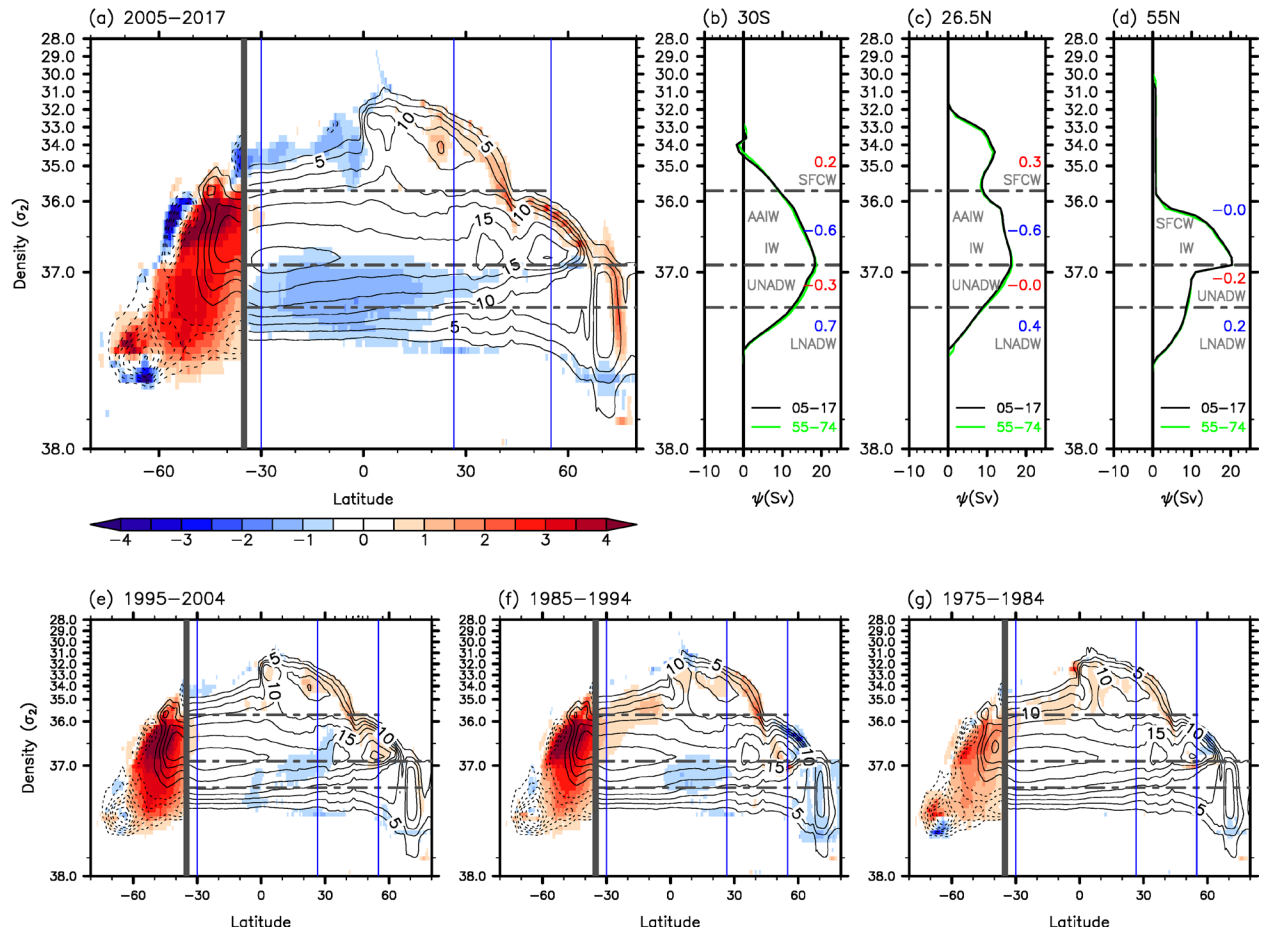
Supplementary Figure 2. The GIOC and its interdecadal changes in the Indo-Pacific and Southern Oceans. The GIOC (contours) in the Southern Ocean (south of 35°S) and the Indo-Pacific Ocean (north of 35°S) and its changes (shades) during (a) 1995-2004, (e) 1985-1994, and (i) 1975-1984 in reference to the base period of 1955-1974. The GIOC at (b,f,j) 65°S and (c,g,k) 43°S in the Southern Ocean, and at (d,h,l) 30°S in the Indo-Pacific Ocean during (b-d) 1995-2004, (f-h) 1985-1994, and (j-l) 1975-1984 (black lines) in reference to those during 1955-1974 (green lines). The vertical axis is potential density in reference to 2,000 m (σ_2 units). The differences in GIOC transport values for SFCW, AAIW, IW, UCDW, LCDW, IDW & PDW, and AABW are shown at (b,f,j) 65°S, (c,g,k) 43°S, and (d,h,l) 30°S. Red color is for the increased transport values, and blue color for the decreased transport values. Volume transports are in Sv units.



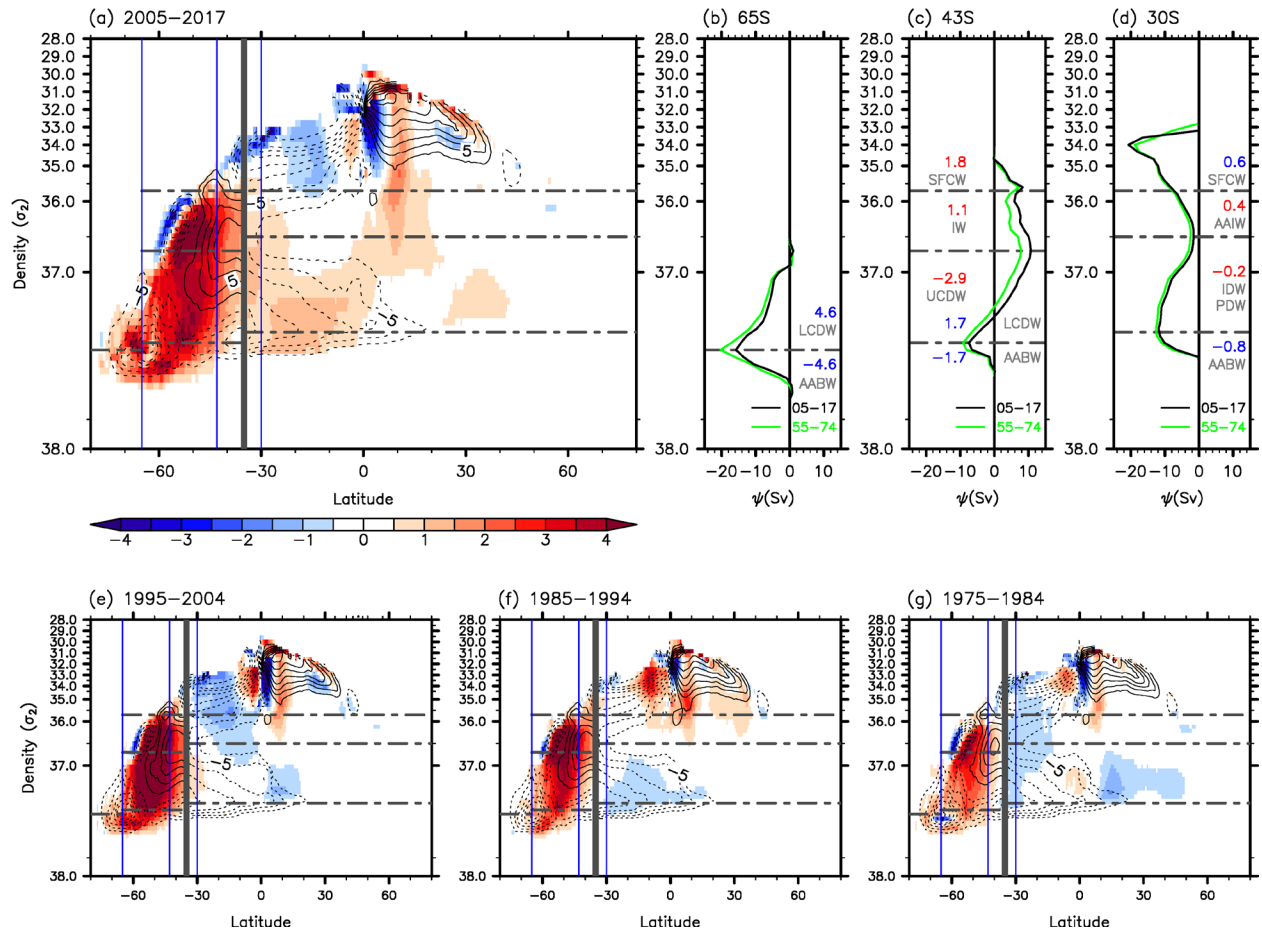
Supplementary Figure 3. The GMOC and its interdecadal changes in the Atlantic and Southern Oceans. The GMOC (contours) in the Southern Ocean (south of 35°S) and the Atlantic Ocean (north of 35°S) and its changes (shades) during (a) 1995-2004, (e) 1985-1994, and (i) 1975-1984 in reference to the base period of 1955-1974. The AMOC at (b,f,j) 30°S, (c,g,k) 26.5°N, and (d,h,l) 55°N during (b-d) 1995-2004, (f-h) 1985-1994, and (j-l) 1975-1984 (black lines) in reference to those during 1955-1974 (green lines). The differences in AMOC transport values for SFCW, AAIW, IW, UNADW and LNADW are shown at (b,f,j) 30°S, (c,g,k) 26.5°N, and (d,h,l) 55°N. Red color is for the increased transport values, and blue color for the decreased transport values. Volume transports are in Sv units.



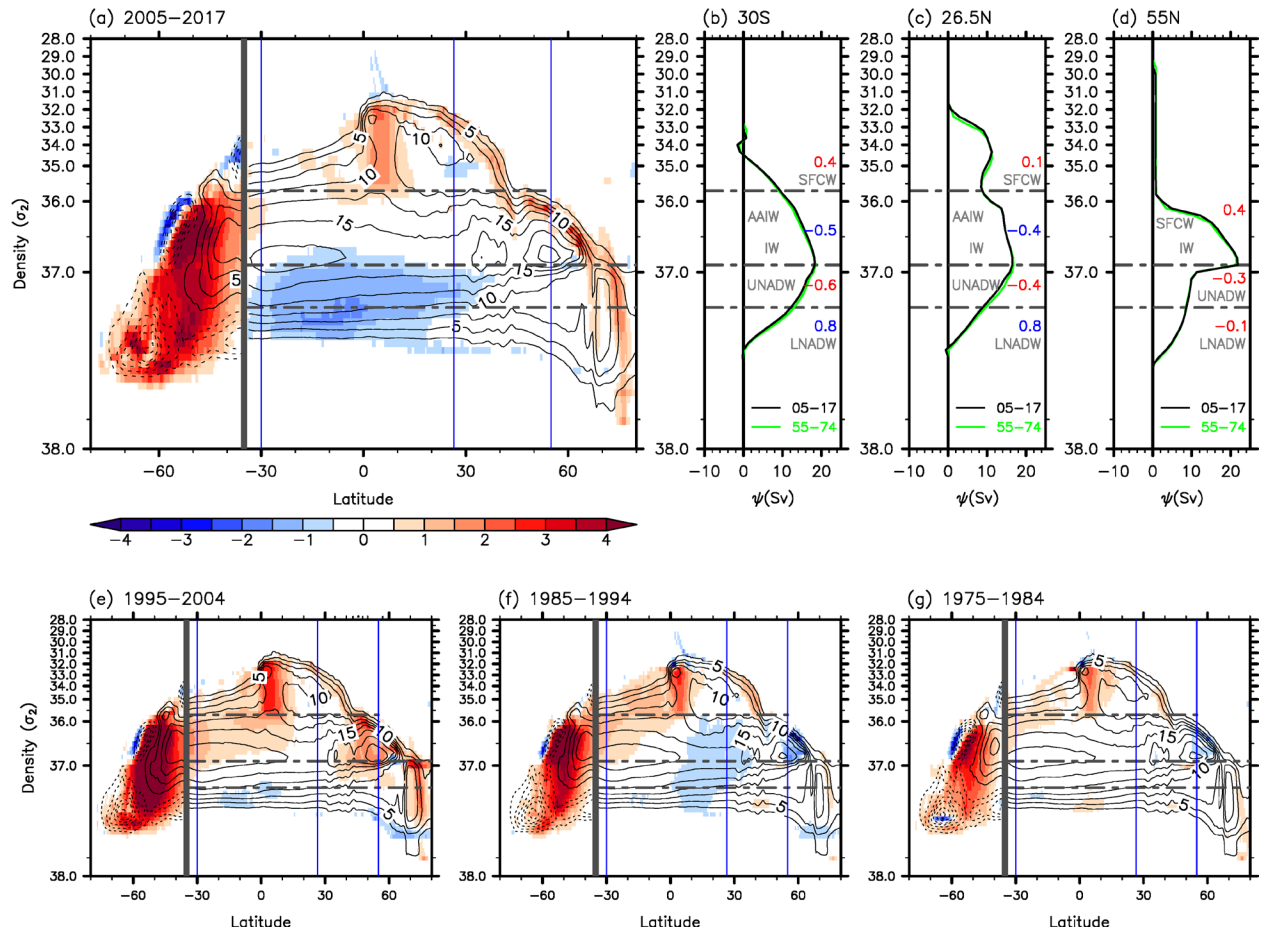
Supplementary Figure 4. Same as Figure 1 except that EN4 data is used instead of WOA18.



Supplementary Figure 5. Same as Figure 2 except that EN4 data is used instead of WOA18.



Supplementary Figure 6. Same as Figure 1 except that JRA55 surface forcing fields are used instead of ERA5 surface forcing fields.



Supplementary Figure 7. Same as Figure 2 except that JRA55 surface forcing fields are used instead of ERA5 surface forcing fields.

Supplementary Table 1. Changes in the GMOC at 65°S, 43°S and 30°S. The differences in overturning transport values between 2005-2017 and 1955-1974 for SFCW, AAIW, IW, UCDW, LCDW, IDW & PWD, and AABW at the core latitudes of the lower and upper overturning cells in the Southern Ocean (i.e., 65°S and 43°S) and at 30°S in the Indo-Pacific Ocean, derived from the three different sets of data-constrained diagnostic ocean model simulations. The mean and standard deviation values derived from the three sets of simulations are also indicated. Red color is for the increased transport values, and blue color for the decreased transport values. Bold values indicate that the mean is larger than the stand deviation. Volume transports are in Sv units.

Hydrography Data	WOA18	EN4	WOA18	Average
Surface Forcing	ERA5	ERA5	JRA55	
<i>65°S (Southern Ocean)</i>				
LCDW	3.3	3.5	4.6	3.8±0.5
AABW	-3.3	-3.5	-4.6	-3.8±0.5
<i>43°S (Southern Ocean)</i>				
SFCW	3.0	3.1	1.8	2.6±0.6
IW	0.5	-0.2	1.1	0.5±0.3
UCDW	-3.5	-2.9	-2.9	-3.1±0.3
LCDW	1.4	1.7	1.7	1.6±0.1
AABW	-1.4	-1.7	-1.7	-1.6±0.1
<i>30°S (Indo-Pacific Ocean)</i>				
SFCW	1.0	1.6	0.6	1.1±0.4
AAIW	0.4	0.5	0.4	0.4±0.0
IDW & PDW	-0.5	-0.9	-0.2	-0.5±0.2
AABW	-0.9	-1.3	-0.8	-1.0±0.2

Supplementary Table 2. Changes in the AMOC at 30°S, 26.5°N and 55°N. The differences in overturning transport values between 2005-2017 and 1955-1974 for SFCW, AAIW, IW, UNADW and LNADW at 30°S, 26.5°N and 55°N in the Atlantic Ocean, derived from the three different sets of data-constrained diagnostic ocean model simulations. The mean and standard deviation values derived from the three sets of simulations are also indicated. Red color is for the increased transport values, and blue color for the decreased transport values. Bold values indicate that the mean is larger than the stand deviation. Volume transports are in Sv units.

Hydrography Data	WOA18	EN4	WOA18	Average
Surface Forcing	ERA5	ERA5	JRA55	
<i>30°S (Atlantic Ocean)</i>				
SFCW	0.1	0.2	0.4	0.2±0.1
IW	-0.6	-0.6	-0.5	-0.6±0.0
UNADW	-0.5	-0.3	-0.6	-0.5±0.1
LNADW	1.1	0.7	0.8	0.9±0.2
<i>25.6°N (Atlantic Ocean)</i>				
SFCW	0.2	0.3	0.1	0.2±0.1
IW	-0.7	-0.6	-0.4	-0.6±0.1
UNADW	-0.3	0.0	-0.4	-0.2±0.2
LNADW	0.8	0.4	0.8	0.7±0.2
<i>55°N (Atlantic Ocean)</i>				
SFCW	0.5	0.0	0.4	0.3±0.2
UNADW	-0.5	-0.2	-0.3	-0.3±0.1
LNADW	0.0	0.2	-0.1	0.1±0.1